Automatic Fabric Defect Detection Using Learning-Based Local Textural Distributions in the Contourlet Domain

Daniel Yapi, Mohand Saïd Allili, *Member, IEEE*, and Nadia Baaziz, *Member, IEEE*

***Abstract*— We propose a learning-based approach for automatic detection of fabric defects. Our approach is based on a statistical representation of fabric patterns using the redundant contourlet transform (RCT). The distribution of the RCT coefficients are modeled using a finite mixture of generalized Gaussians (MoGG), which constitute statistical signatures distinguishing between defective and defect-free fabrics. In addition to being compact and fast to compute, these signatures enable accurate localization of defects. Our defect detection system is based on three main steps. In the first step, a preprocessing is applied for detecting basic pattern size for image decomposition and signature calculation. In the second step, labeled fabric samples are used to train a Bayes classifier (BC) to discriminate between defect-free and defective fabrics. Finally, defects are detected during image inspection by testing local patches using the learned BC. Our approach can deal with multiple types of textile fabrics, from simple to more complex ones. Experiments on the TILDA database have demonstrated that our method yields better results compared with recent state-of-the-art methods.**

***Note to Practitioners*—Fabric defect detection is central to automated visual inspection and quality control in textile manufacturing. This paper deals with this problem through a learning-based approach. By opposite to several existing approaches for fabric defect detection, which are effective in only some types of fabrics and/or defects, our method can deal with almost all types of patterned fabric and defects. To enable both detection and localization of defects, a fabric image is first divided into local blocks, which are representative of the repetitive pattern structure of the fabric. Then, statistical signatures are calculated by modeling the distribution of coefficients of an RCT using the finite MoGG. The discrimination between defect-free and defective fabrics is then achieved through supervised classification of RCT-MoGG signatures based on expert-labeled examples of defective fabric images. Experiments have shown that our method yields very good performance in terms of defect detection and localization. In addition to its accuracy, inspection of images can be performed in a fully automatic fashion, whereas only labeled examples are initially required. Finally, our method can be easily adapted to a real-time scenario since defect detection on inspected images is performed at the block level, which can be easily parallelized through hardware implementation.**

Manuscript received November 10, 2016; revised March 3, 2017; accepted April 11, 2017. This paper was recommended for publication by Associate Editor Y. Zhang and Editor Y. Sun upon evaluation of the reviewers' comments. This work was supported by the Natural Sciences and Engineering Research Council of Canada. *(Corresponding author: Mohand Saïd Allili.)*

The authors are with the Department of Computer Science and Engineering, Universite du Quebec en Outaouais, Gatineau, QC J8X 3X7, Canada (e-mail: mohandsaid.allili@uqo.ca).

Color versions of one or more of the figures in this paper are available online at http://ieeexplore.ieee.org.

Digital Object Identifier 10.1109/TASE.2017.2696748

***Index Terms*— Bayes classifier (BC), contourlet transform, fabric defect detection, mixture of generalized Gaussians (MoGG), texture analysis.**

I. Introduction

TEXTILE is used in multiple products such as clothing, filters, wipes, and in housing and transportation materials. However, the presence of defects in fabrics can reduce prices with losses reaching 45%–65% [21]. To enhance the efficiency of fabric defect detection, it is necessary to replace the fastidious manual inspection with automatic inspection for better productivity and improving quality of fabric as well (see Fig. 1 as an example for automatic inspection systems). Automated defect detection of fabrics reduces the labor cost and enables to cover a broader range of different fabrics, from homogenous texture to the most complex one. Currently, there exist more than 70 established categories for fabric defects defined by the textile industry [36]. Most of these defects are caused by machine malfunctions, yarn problem, and stain of oil caused by the knitting device, among others.

Fabric can be considered as a 2-D patterned texture [36], [55]. All fabrics can be classified into the 17 established wallpaper groups denoted by $p1$, $p2$, $p3$, $p3m1$, $p31m$, $p4$, $p4m$, $p4g$, pm, pg, pmg, pgg, $p6$, $p6m$, cm, cmm, and pmm, which are lattices composed of elementary elements called *motifs*, which are organized repetitively along parallelogram, rectangular, rhombic, square, or hexagonal shapes [13]. The $p1$ group defines a texture with just one fundamental lattice repeating itself over the complete fabrics such as plain, twill, and plain weave fabrics (see Fig. 2 for illustration). This group involves only pattern translations. The other groups involve one or more other types of symmetries such as rotations, reflections, and glide reflections (see Fig. 3 for illustration). Considering the classification of inspected fabric types, Ngan *et al.* [36] have proposed a taxonomy for defect detection methods, which broadly categorizes the methods into two main groups. The first group of methods (nonmotif-based) do not take into consideration the basic motif distribution for fabric inspection. They rely instead on analyzing textural properties of fabric images. These methods can, therefore, deal with fabrics of type $p1$ (e.g., plain and twill) as well as with other types of fabrics in the wallpaper groups. The second group of methods (motif-based) relies on the analysis of the structure of the fabric basic motifs to detect potential defects. Since it is very difficult to model statistically/geometrically the distribution of basic motifs in these groups, methods use

Fig. 1. Example of an automated inspection machine for textile fabric.

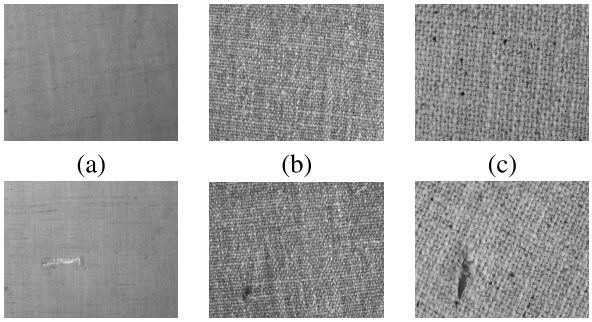

Fig. 2. Fabric images from TILDA database representing the $p1$ wallpaper group. (a) Plain fabric without defects. (b) Twill fabric without defects. (c) Plain weave fabric without defects. (d) Plain fabric with defects. (e) Twill fabric with defects. (f) Plain weave fabric with defects.

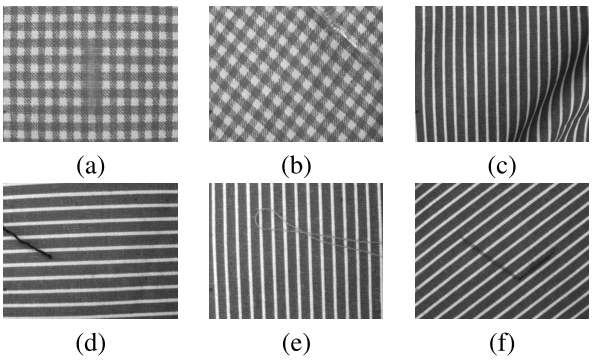

Fig. 3. Non-$p1$ wallpaper group fabric images in the TILDA database. (a) Gingham fabric ($p4m$). (b) Gingham oblique fabric. (c) Fabric with vertical stripes ($p2$). (d) Fabric with horizontal stripes. (e) Fabric with vertical stripes. (f) Fabric with oblique stripes.

mainly pattern matching and image subtraction to localize potential defects [35].

Several fabric defect detection methods have been proposed in the last three decades [11], [21], [36]. The majority of these methods is specific to the nonmotif-based category and deal mainly with fabrics of type $p1$ [22], [31], [32], [34], [43], [48]. Recently, some approaches have been proposed for motif-based defect detection [34], [35]. These have been evaluated mainly on texture patterns of $p1$ and pmm fabric types. However, they do not generalize well for other types of fabric. In addition, these methods detect defects at the image level (i.e., an image contains a defect or not) and do not provide defect details at the lattice or motif level. To resolve the above limitations, Kuo *et al.* [22], [33] have proposed generic methods that can be applied to multiple types of fabrics to localize the defects. These methods are often based on template-matching (TM) or statistical techniques that compare the inspected fabric with the defect-free reference one to detect defects [31], [36]. Ngan *et al.* [33] have proposed to analyze the energy of motif subtraction to detect defects. This method can be applied to 16 of the 17 wallpaper groups and has shown some robustness to noise and slight motif shift. However, it requires a defect-free ground truth to compare the motifs. In addition, it uses a circular shift to perform image subtraction, which incurs a huge computation time. Ng *et al.* [31] have used energy minimization to decompose an image into two structures: a cartoon image representing the defect and the texture structure representing the repetitive patterns. This method yields very good results for defect localization and can be applied practically to all fabric types. However, it requires the inspected image to be perfectly aligned with the ground truth. In addition, it is not efficient for detecting defects with small contrast in the image (e.g., oil stains).

In this paper, we introduce a novel defect detection algorithm that has the capability to cope with different types of defects in the $p1$ and non-$p1$ groups. Therefore, our method can be considered as a hybrid one since it relies mainly on analyzing texture patterns for fabric defect detection. Strictly speaking, our method does not consider elementary motifs as a basic manipulation unit [36]. Instead, it decomposes the image into elementary repetitive units (ERUs) characterized by their periodicity along the fabric lattice. Contrarily to analyzing the fabric at the image level [31] or using the basic motifs [36], ERUs constitute an intermediate representation coarsely describing the local structure of the texture to allow an analysis similar to methods of type $p1$ group to be performed. Each ERU undergoes first a multiscale contourlet decomposition describing local directional and structural properties of the fabric texture. A statistical signature of the mixture of generalized Gaussian distributions (MoGG) is then calculated on the contourlet coefficients [3], [6], which constitute our representation for fabric comparison. Given a set of labeled samples of signatures representing defect-free and defective fabric ERUs, we train a Bayes classifier (BC) to separate between defect-free and defective fabrics, which is then applied to inspect new images for defect detection. Experiments conducted on the TILDA database [45] have shown that the proposed algorithm yields better results compared with other previous works. The main contributions of our work in this paper can be summarized in the following points.

1) A generalized nonmotif-based method is proposed for fabric defect detection. Our method not only can deal with the $p1$ fabric group but also with other fabric groups. It relies on an intermediate representation of fabrics using ERUs, which facilitates local inspection of images with complex patterns and enables accurate localization of defects.
2) To describe fabric texture structure, we use multiscale contourlet decomposition [redundant contourlet transform (RCT)] and MoGG, which allow robustness to noise and nonuniform illumination. It has also invariance to fabric translation and scale changes. These descriptors

calculated on the ERUs are called RCT-MoGG signatures.

3) Our defect detection method is based on a learning-based approach that separates RCT-MoGG signatures of defect-free and defective fabrics using a set of learning examples with their ground truth. After decomposing a fabric image into ERUs, a classification of the ERU blocks is performed to assess whether each ERU is defect-free or contains defects. Our method provides an overall high detection accuracy and very low false alarm rate (FR) compared with recent state-of-the-art methods.

The remainder of this paper is organized as follows. Section II presents a brief literature review on fabric defect detection methods. Section III presents our method for automatic defect detection. Section IV presents some experimental results. We end this paper with the conclusion.

II. Related Work

The majority of existing works on fabric inspection is related to the *nonmotif-based* category of methods [21]. These methods have been designed for the simplest patterns of the $p1$ homogenous fabrics [7], which include plain and twill fabrics. Proposed *nonmotif-based* methods can be classified into four main approaches: 1) *statistical*; 2) *spectral*; 3) *model-based*; and 4) *learning-based* approaches [36]. Compared with the *nonmotif-based* category, a small number of methods have been proposed for the *motif-based* one [33].

A. Inspection Approaches for the p1 Fabrics

Statistical methods include mainly the analysis of *the autocorrelation function* (AF) and the cooccurrence matrix (CM) [10], [52]. The AF has been applied to detect fabric defects by assuming that autocorrelation maxima stay constant for repetitive patterns with perfect replication throughout the fabric [10], [25]. In the same vein, the AF is applied to describe translational and rotational symmetry in plain fabric images [52]. This approach although interesting has not been evaluated by explicit performance metrics on fabric defects [36]. Wood [52] has used features calculated from the CM to classify fabrics as normal or defective using neural networks. Likewise, Amet *et al.* [5] have applied CM analysis in the wavelet domain to detect defects. In [20], CM features are fed into a neural network to detect defects at the pixel level. The major limitation of using CM features is that they incur a huge computation time for their calculation. In addition, since CM computing is based on adjacent pixels analysis, CM features can be sensitive to scale changes in the fabric texture.

Spectral approaches consist of locating defects in spectral domain [21]. These approaches include the Fourier transform (FT) [9], [47], the wavelet transform (WT) [41], [53], [54] and the Gabor transform [18]–[20]. The main drawback of using the FT is that it lacks local support (i.e., lack of information support in the spatial domain), which can prevent it from detecting defects in random patterned texture such as twill and plain fabrics. Contrary to the FT, wavelet and Gabor filters make use of a spatial frequency analysis, which enables them to detect local defects. For instance, Chin and Harlow [10] have proposed a wavelet-based approach to detect defects on plain and twill fabrics. They reported a detection success rate of 97.5%, but the method is computationally intensive.

Model-based approaches address the defect detection problem by fitting parametric models to feature distribution of the fabric [21], [30]. Inspired by existing works on texture modeling, Cohen *et al.* [12] have used Gaussian Markov fields (GMFs) to model defect-free texture on fabric images. In the same vein, Ozdemir and Ercil [37] have applied Markov random fields (MRFs) for fabric inspection. Although GMFs and MRFs are good for extracting local contextual information of texture patterns, they are not efficient in detecting small defects. In addition, these methods are computationally intensive. To exploit linear dependency between pixels, Serafim [28] has used autoregressive models to detect defects on leather surfaces. Although this method can operate in a real-time scenario, it is sensitive to the size of defects and nonuniform illumination.

Learning-based approaches use labeled samples to train classifiers that assign images to defective or defect-free classes. For instance, Kuo and Lee [24] have used backpropagation neural networks for defect detection. They achieved very good detection rates on defective samples of plain fabric. This method, however, does not generalize well to other types of fabric and it is computationally intensive. Sezer *et al.* [42] have used independent component analysis (ICA) on a sample of images to detect defects at the block level of fabrics. This approach has yielded good results on uniform textures (plain fabric). However, it does not generalize well for irregular random textures (e.g., twill and plain weave textures).

B. Inspection Approaches for the Non-p1 Fabrics

These are also named *hybrid approaches* since they use a combination of techniques for defect detection on fabrics in the $p1$ and non-$p1$ groups [36]. They can be broadly classified as TM and statistical/spectral approaches. Approaches using TM use image subtraction methods to compare inspected fabric with defect-free ones [33]. Kuo and Su [22] have proposed a method using features calculated from the CM and correlation analysis to detect defects. This method has been successfully applied to Jacquard fabrics belonging to the $p2$ group. However, CM features are highly sensitive to small variation or misalignment in patterns and their calculation is computationally prohibitive. Tajeripour *et al.* [44] have proposed a method based on local binary patterns (LBPs) and adaptive thresholding for defect detection. The LBP technique has been first proposed for texture description and has good properties for rotation invariance and multiscale analysis. This method has shown good results for $p1$ and several non-$p1$ groups, but it may yield too many false positives (FPs) for erroneous thresholds. Besides, the size of the windrow is not adaptable since it is always fixed to 16×16.

Direct thresholding [32] has been used for the analysis of horizontal and vertical sub-bands of the Haar WT for defect detection. This method named wavelet golden image subtraction is computationally fast and leads to good performance on several types of fabrics. However, the calculated thresholds can be hard to determine for some fabrics like charter-box pattern. Recently, Tsang *et al.* [48] have proposed a fabric

inspection method based on the Elo rating formalism [15]. This method can effectively deal with non-$p1$ fabric groups like dot-patterned (pmm group) and star-patterned ($p2$ group) and box-patterned fabrics ($p4m$ group). However, it showed weak generalization to other types of fabric. Bollinger bands, originally introduced for financial analysis, have been successfully applied for defect detection in fabric groups $p2$, pmm, and $p4m$ [34]. But defects near the image border or smaller than one repetitive unit may not be detected by the method.

Recently, Ng *et al.* [31] have proposed an energy minimization method for decomposing an image into defect and normal fabric images. This method can be applied for several types of fabrics. However, the method can be very sensitive to noise, defect contrast, and errors of alignment between reference (defect-free) and inspected fabrics. Finally, sparse coding (SC) is another successful technique that has been used for defect detection [56], [57]. SC aims at approximating an input signal as a linear combination of a few components selected from a dictionary of basic elements called *atoms* [26]. Zhou and Wang [57] have proposed using SC for defect-free fabric reconstruction. Thus, reconstruction error acts as an indicator for the presence of defects in an inspected fabric. The major limitation of the method, however, is its computation time and weak robustness to noise. To reduce the noise effect, Gabor filters can be used before applying the SC technique as proposed in [58]. They have reported a significant improvement on plain, twill, and plain weave fabrics from the Tilda data set [45].

C. Motif-Based Methods

Among recent studies for defect detection, only few papers consider elementary fabric motifs as a basic manipulation unit [36]. Ngan *et al.* [33], [35] are among recent works falling into this category of methods. They try to handle explicitly fabrics in the non-$p1$ groups and use symmetry properties of motifs to calculate the energy of moving subtraction and its variance among motifs. Decision boundaries are determined by learning the distribution of those values among the defect-free and defective patterns in the energy-variance space [33]. An extensive performance evaluation on defects in 16 out of 17 wallpaper groups has achieved an overall detection success rate of 93.86%. However, the method is computationally intensive because too large database of defect-free and defective samples is needed for training. Besides, it uses a decision boundary (a sort of threshold), which requires to be manually set for each fabric to guarantee good results, and thus the method is not easy to generalize to all types of fabric. To isolate defects on fabric images, Jing *et al.* [17] have proposed to subtract a golden template from a filtered fabric image using Gabor filters. The method has shown good results for defect detection and localization on patterned fabrics. However, it can be sensitive to noise and nonuniform illumination, which increase the amount of FPs. In addition, because of the difficulty of calculating the golden image template, the performance decreases for irregular patterned fabrics.

III. Proposed Approach for Defect Detection

The proposed method aims at developing a principled methodology ensuring full automation of defect detection while enabling to efficiently cope with several types of fabrics and defects. As stated before, our approach is composed of three basic steps. In the first step, a preprocessing is used to determine the ERUs for image decomposition. The second step consists of calculating statistical signatures on labeled samples of fabric images. This step also involves training a BC to discriminate between defective and nondefective fabrics. In the third and final step, images of inspected fabrics are passed through the signature generator and the BC to detect potential defects. In what follows, we give details about each of the above steps separately.

A. Image Decomposition Into ERUs

To make our approach generalizable to multiple fabric groups, we use an intermediate representation of the fabric called an ERU. In a nutshell, an ERU can be considered as a super motif, which enables dealing with non-$p1$ fabric group using methods of type $p1$ group. We calculate these units by analyzing texture patterns of the fabrics using the AF on the fabric image.

Let I be a fabric image of size $n \times m$. We denote by $I_{\text{hs}}(i)$ the image resulting from using i horizontal circular shifts for the image I. Likewise, we denote by $I_{\text{vs}}(j)$ the result of using j vertical circular shifts for I. The size of a repetitive pattern (i.e., period) is determined by peaks of the AF of the image I that can be calculated using the original I and its shifts in the horizontal and vertical directions, respectively. The following functions can be used to compute the size of the period in the two directions:

$$\begin{cases} h' &= \arg\max_{1 \le i < n} \{N(I) \circ N(I_{\text{hs}}(i))\} \\ w' &= \arg\max_{1 \le j < m} \{N(I) \circ N(I_{\text{vs}}(j))\} \end{cases} \tag{1}$$

where $N(\cdot)$ is a function having the role of normalizing and putting an image in a vector form. The operator $\circ$ indicates the correlation function between vectors. Basically, (1) determines the horizontal and vertical dimensions of the repetitive pattern. Finally, to enable robust RCT decomposition and MoGG parameter estimation, we should maintain a minimum size of the ERU such that a sufficient number of pixels are contained in the unit. By taking δ as the minimum size of each side of an ERU, the optimal height and width of an ERU are given by $\mathbf{h} = k_h \cdot h'$ and $\mathbf{w} = k_w \cdot w'$, such that $k_h = \{\arg\min_k (k \cdot h') | k \cdot h' \geqslant \delta\}$ and $k_w = \{\arg\min_r (r \cdot w') | r \cdot w' \geqslant \delta\}$, where $k, r \in \mathbb{N}^*$. Fig. 4 gives some examples of ERU calculation on fabric images where the parameter δ is set to 64. We can note that the periodic patterns have been clearly identified using our method.

Once the size of the ERU is determined, the image is divided into blocks, which are used to calculate the statistical signatures for defect detection. In other words, taking the detected ERU as an elementary fabric motif, any fabric can be brought to the $p1$ group, since the only transformation undergone by the ERUs consists of horizontal and vertical translations. Note that having an ERU for each fabric image incurs that before analyzing inspected fabric for defect detection, it must be decomposed into ERUs in the same way as the reference fabric. Consequently, in order to have a comparable ERU, a

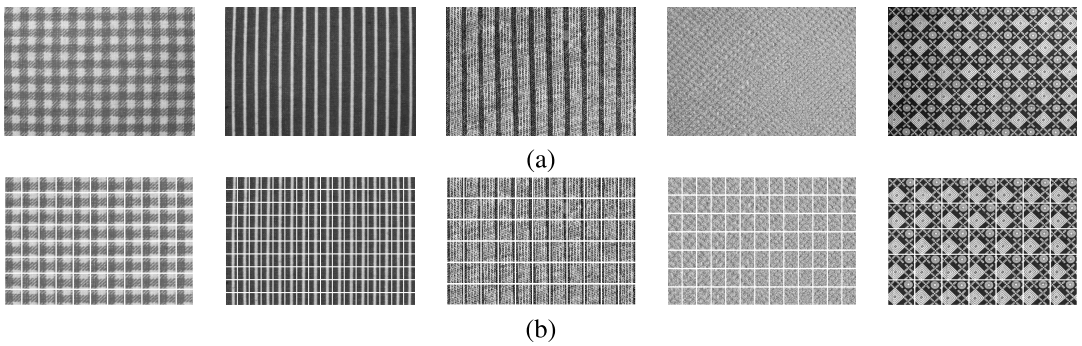

Fig. 4. Illustration of ERU calculation for some fabric samples. (a) Original fabric. (b) Image grid with ERUs.

preprocessing step might be required to align the inspected image with the reference one.

B. MoGG Modeling for Redundant Contourlet Transform

The standard contourlet transform (SCT) has been proposed [14] to improve the representation of texture over wavelets. Later on, the RCT has been proposed as an alternative to the SCT [6] to overcome the limitation due to subsampling in the SCT. In addition to having the good properties of the SCT, the RCT reduces the decimation, avoids the multiscale interpolation in the SCT, and enables easy correspondence between the different levels of image resolutions. The RCT shares the same decomposition scheme with the SCT. However, all downsampling operations in the RCT are discarded from the Laplacian stage and a set of symmetric low-pass filters having adequate frequency selectivity and pseudo-Gaussian properties are employed. Filter impulse responses $g_b(s)$, as given in the following, are finite and symmetric:

$$g_b(s) = e^{-2\frac{s}{b}} - e^{-2}\left(e^{-2\left(\frac{s-b}{b}\right)^2} e^{-2\left(\frac{s+b}{b}\right)^2}\right) \tag{2}$$

where s is the spatial row/column location and b is a factor influencing the frequency bandwidth. Using L filters (with $b = 2^{\ell}$, $\ell \in \{1, 2, \ldots, L\}$) results in a redundant Laplacian pyramid (RLP) having $L + 1$ equal-size subimages: one coarse image approximation and L bandpass subimages. Then, a directional filter bank with $D = 4$ orientations and 1:4 critical downsampling is applied on each of the L RLP sub-bands to obtain $4L$ equal-size directional sub-bands ($C_{ld}, l = 1, \ldots, L; d = 1, \ldots, D$) in addition to a 1:4 downsampled image approximation C_L. The RCT has been successfully used in [2] and [4] for texture retrieval and defect detection on plain fabrics.

In this paper, we use the RCT for describing the texture structure of several types of fabrics, from the $p1$ to the non-$p1$ groups. More specifically, let $x_1, \ldots, x_n$ be the produced RCT coefficients at a given sub-band after decomposition. Since the distribution of these coefficients can be multimodel, we propose to model this distribution using an MoGG [1], [8]. By supposing a mixture of K components, the marginal distribution of the coefficient variable $\mathbf{x} \in \mathbb{R}$ is given by

$$p(x|\Theta) = \sum_{i=1}^{K} \pi_i \, p(x|\theta_i) \tag{3}$$

where $\theta_i = \{\mu_i, \sigma_i, \beta_i\}$ and π_i, $i = 1, \ldots, K$, are the mixing parameters, with $0 < \pi_i \leq 1$ and $\sum_{i=1}^{K} \pi_i = 1$. Each component of the mixture is modeled using a general Gaussian distribution (GGD): $p(x|\theta_i) = ((C(\beta_i))/(2\sigma_i))\exp(-A(\beta_i)|(x - \mu_i)/\sigma_i|^{\beta_i})$, where $A(\beta_i) = [((\Gamma(3/\beta_i))/(\Gamma(1/\beta_i)))]^{((\beta_i)/(2))}$, $C(\beta_i) = \beta_i(((\Gamma(3/\beta_i))/(\Gamma(1/\beta_i))))^{1/2}/\Gamma(1/\beta_i)$, and $\Gamma(\cdot)$ denotes the Gamma function. The parameters μ_i and σ_i denote the distribution mean and standard deviation, respectively. The parameter β_i is the shape parameter, which fits the kurtosis of the ith GGD and determines whether the distribution is peaked or flat. The details of parameter estimation of the MoGG are given in [3]. We use a Bayesian estimation to learn the model parameters θ_i, $i = 1, \ldots, K$, whereas the minimum message length principle is applied for selecting the best value of the parameter K [51].

Fig. 5 shows a comparison of the RCT-MoGG signatures of two blocks in the same fabric [Fig. 5(a)]: a defect-free block (green) and a defective one (red). Note first that the shape of coefficients histogram can be sharply peaked, heavy tailed, and slightly asymmetric. Thanks to its flexibility, the MoGG has enabled to precisely fit to the different shapes. We can also note the discrepancy between the signatures of defective and defect-free blocks for both high- and low-pass sub-bands. This makes the RCT-MoGG description a very efficient tool to assess about defects present in the fabric.

C. Similarity Measurement for Defect Detection

Do and Vetterli [14] have used a closed-form Kullback–Leibler divergence (KLD) to measure similarity between two statistical distributions of wavelet sub-band coefficients. When these distributions are multimodal, a closed-form solution is intractable [3]. To circumvent this issue, we resort to approximating the KLD using Monte Carlo sampling methods, as proposed in [4]. Given two MoGG models $P(x) = \sum_{i=1}^{K} \pi_i \, p(x|\theta_i)$ et $Q(x) = \sum_{j=1}^{M} \omega_j q(x|\theta_j)$, the KLD between these models is defined as follows:

$$\mathrm{KLD}(P||Q) = \int P(x) \log\left(\frac{P(x)}{Q(x)}\right) dx. \tag{4}$$

The KLD by Monte Carlo integration is given by

$$\mathrm{KLD}_{\mathrm{mc}}(P||Q) = \frac{1}{n}\sum_{i=1}^{n} \log\frac{P(x_i)}{Q(x_i)} \approx \mathrm{KLD}(P||Q). \tag{5}$$

The Monte Carlo method aims at generating a sufficiently large sample $\mathcal{X} = \{x_1, x_2, \ldots, x_n\}$ drawn independently from the

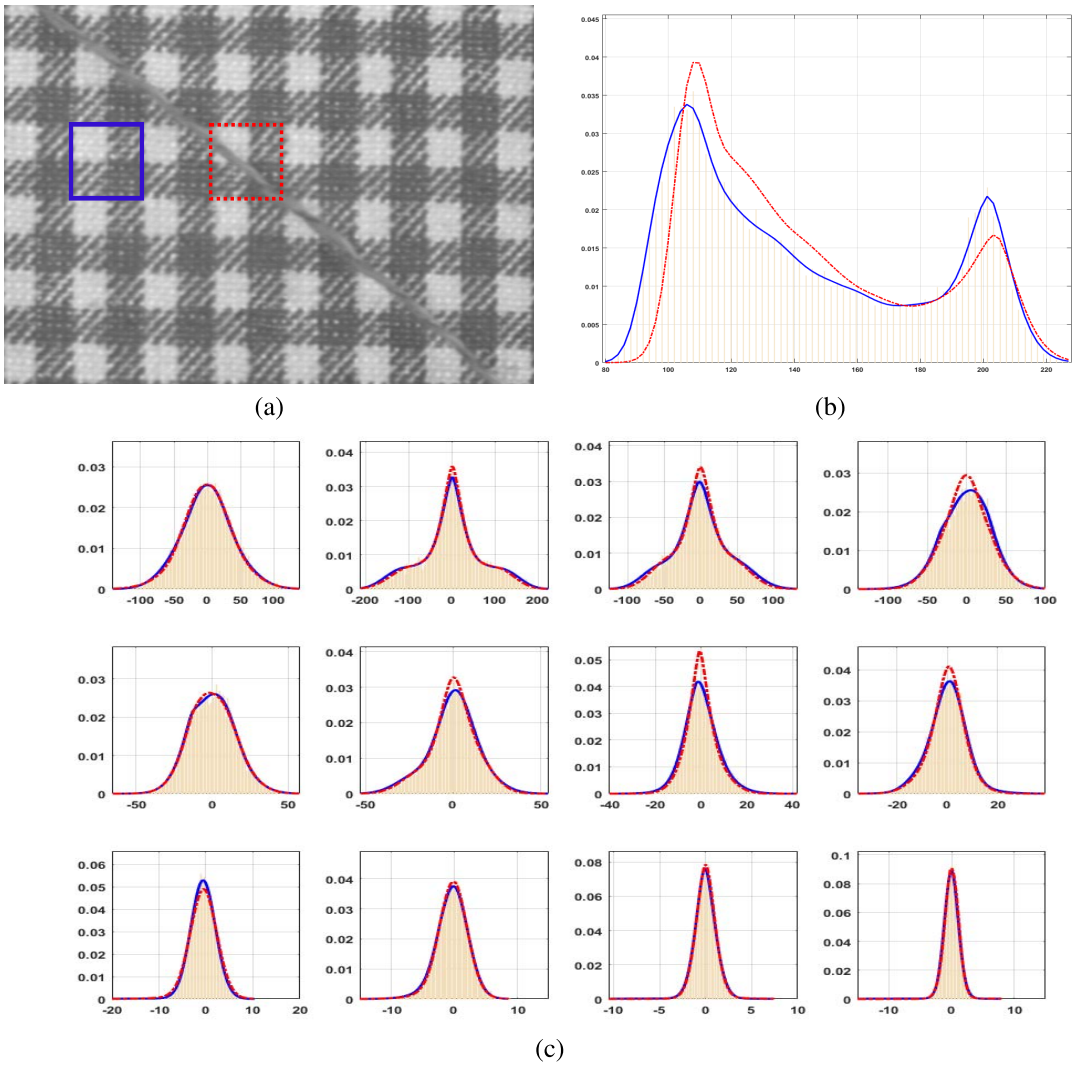

Fig. 5. RCT-MoGG signature calculation for defective and defect-free fabrics. (a) Examples of defective (dashed red square) and defect-free (solid blue square) blocks. (b) and (c) Yellow histograms of low- and high-pass RCT coefficients of the defect-free block in (a). The dashed red and solid blue lines show MoGG signatures of the defective and defect-free blocks, respectively. (c) Four directional decompositions (left to right) and levels 1–3 of the RCT-MoGG signatures, respectively (top to bottom).

distribution P to approximate the KLD integration [40]. We used $n = 10^4$ as a typical value that gives satisfactory results.

D. Learning-Based Defect Detection Algorithm

The flow diagram for our algorithm is shown in Fig. 6. As mentioned previously, our approach works into two stages: *a learning phase*, in which a BC is trained on a set of labeled fabric examples, and an *inspection phase*, which uses the trained classifier on a set of newly seen images to detect potential defects. Our algorithm operates at the block level of images, which aims at localizing defects at fine resolutions allowed by the ERU decomposition.

1) Learning Stage: Let $\mathcal{T} = \mathcal{B} \cup \tilde{\mathcal{B}}$ be the set of training examples composed of two subsets $\mathcal{B} = \{B_1, \ldots, B_n\}$ and $\tilde{\mathcal{B}} = \{\tilde{B}_1, \ldots, \tilde{B}_m\}$, containing defect-free and defective blocks, respectively. For each block in $\mathcal{T}$, we calculate its RCT-MoGG signature, which combines several orientations and scales of the texture. The training process of the defect detection system is given by the script of Algorithm 1. The algorithm trains a BC and results in a set of reference blocks $\mathcal{R}$ that will be used to inspect newly-seen textile images. The set $\mathcal{R}$ is a sort of a landmark signature that contains the different configurations and patterns of the textile type to be inspected.

The training process iterates on the sets $\mathcal{B}$ and $\tilde{\mathcal{B}}$ by choosing at each time a new reference block to add to the set $\mathcal{R}$. The first reference block $B_{r_1} \in \mathcal{R}$ can be chosen randomly from $\mathcal{B}$. After calculating the KLDs of all the training blocks with B_{r_1}, we obtain the sets $\mathcal{D} = \{d_1, \ldots, d_n\}$ and $\tilde{\mathcal{D}} = \{\tilde{d}_1, \ldots, \tilde{d}_m\}$ for $\mathcal{B}$ and $\tilde{\mathcal{B}}$, respectively. Then, we train a BC on $\mathcal{D} \cup \tilde{\mathcal{D}}$, where a Gaussian $P_{\mathcal{B}}$ ($P_{\tilde{\mathcal{B}}}$) is fitted to class $\mathcal{B}$ ($\tilde{\mathcal{B}}$). After classifying the training blocks using BC, we obtain the classification error ε (i.e., the number of badly classified blocks) and the set $\mathcal{C}$ of false defect detections (i.e., blocks in $\mathcal{B}$ classified as defect by BC).

To augment the set $\mathcal{R}$ with a new reference block, we search for a block in $\mathcal{C}$ corresponding to either the median or the maximum of distances in $\mathcal{C}$. Using the new set $\mathcal{R}$, we update the distances $\mathcal{D}$ and $\tilde{\mathcal{D}}$ as follows. Let B_k be a block in $\mathcal{T}$ and $\mathrm{KLD}_{r_1}, \ldots, \mathrm{KLD}_{r_N}$ are the set of KLDs calculated with all reference blocks in $\mathcal{R}$, where N is the cardinality of $\mathcal{R}$. The

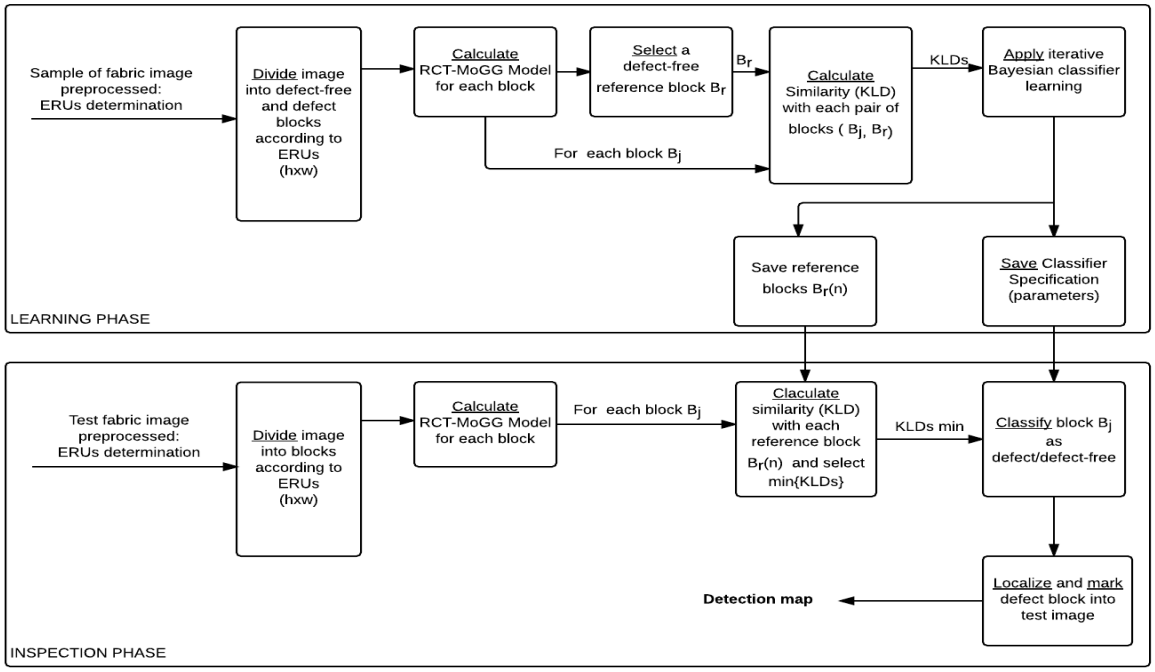

Fig. 6. Block diagram of the proposed defect detection method.

Algorithm 1: Defect Detection Learning Phase

Data: $\mathcal{B} = \{B_1, \ldots, B_n\}$ and $\tilde{\mathcal{B}} = \{\tilde{B}_1, \ldots, \tilde{B}_m\}$.
Result: Set of reference blocks: $\mathcal{R}$, Bayes classifier: BC.
Generate RCT-MoGG signature for each block in $\mathcal{B}$ and $\tilde{\mathcal{B}}$
$\mathcal{R} \leftarrow B_1$; $\varepsilon \leftarrow \infty$; $\mathcal{C} \leftarrow \emptyset$; $N \leftarrow 0$;
repeat
1- $N \leftarrow N + 1$;
2- $\varepsilon_p \leftarrow \varepsilon$;
3- Update the set $\mathcal{R}$ from $\mathcal{C}$;
4- Calculate the KLDs $\{d_1, \ldots, d_n\}$ and $\{\tilde{d}_1, \ldots, \tilde{d}_m\}$;
5- Train a Bayes classifier on the KLDs;
6- Classify the ERUs and calculate the error ε;
7- Update $\mathcal{C}$ the set of false defect detections;
until ($\varepsilon = 0$ OR $\varepsilon \geq \varepsilon_p$)

Algorithm 2: Inspection for Defect Detection

Data: Input image I, $\mathcal{R} = \{B_{r_1}, \ldots, B_{r_N}\}$ and the BC.
Result: Image with blocks classified.
Decompose the image into blocks;
Generate RCT-MoGG signature for each block;
for (each block B_k) **do**
1- Calculate the KLDs $\{KLD_{r_1}, \ldots, KLD_{r_N}\}$;
2- Choose $d_k = \min\{KLD_{r_1}, \ldots, KLD_{r_N}\}$;
3- Use BC to classify B_k.
end for

new KLD assigned to the block for the next iteration (Step 2 of the algorithm) is given by $d_k = \min\{\text{KLD}_{r_1}, \ldots, \text{KLD}_{r_N}\}$ and a new BC is trained with the new sets $\mathcal{D}$ and $\tilde{\mathcal{D}}$. This process is repeated until the classification error ε is null or higher than ε_p, the classification error at previous iteration. The threshold ε_p is set experimentally using cross validation.

2) Inspection Phase: The inspection phase is performed on a newly seen textile image of the same type as the one used in the learning phase. The steps of the inspection process are given in the script of Algorithm 2. First, the input textile image is decomposed into blocks with the same dimension as the training ones. Each block is then classified as containing defects or defect-free using the reference set $\mathcal{R}$ and the trained BC. Note that in order to achieve very precise localization of defects, image subdivision into blocks may be performed with overlapping.

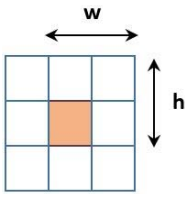

Fig. 7. Illustration of block overlapping for enhancing defect localization. In this example, the resolution of defect detection is half the size of an ERU.

3) Enhancing Defect Localization: A straightforward idea to enhance the defect localization is to reduce the block size. However, this cannot be achieved by our method since a minimal size of data is required to have stable RCT-MoGG signatures [3]. In fact, the RCT cannot be calculated for images under a minimal size of 64×64 [6]. In addition, significance of statistical parameters for the MoGG models is dependent on the number of data [29], [39].

To enhance the precision of defect localization without affecting the quality of RCT-MoGG signatures, we devise a new procedure based on subdividing the image into blocks using an appropriate overlapping as illustrated in Fig. 7. This allows for each block to cast one vote for all its contained

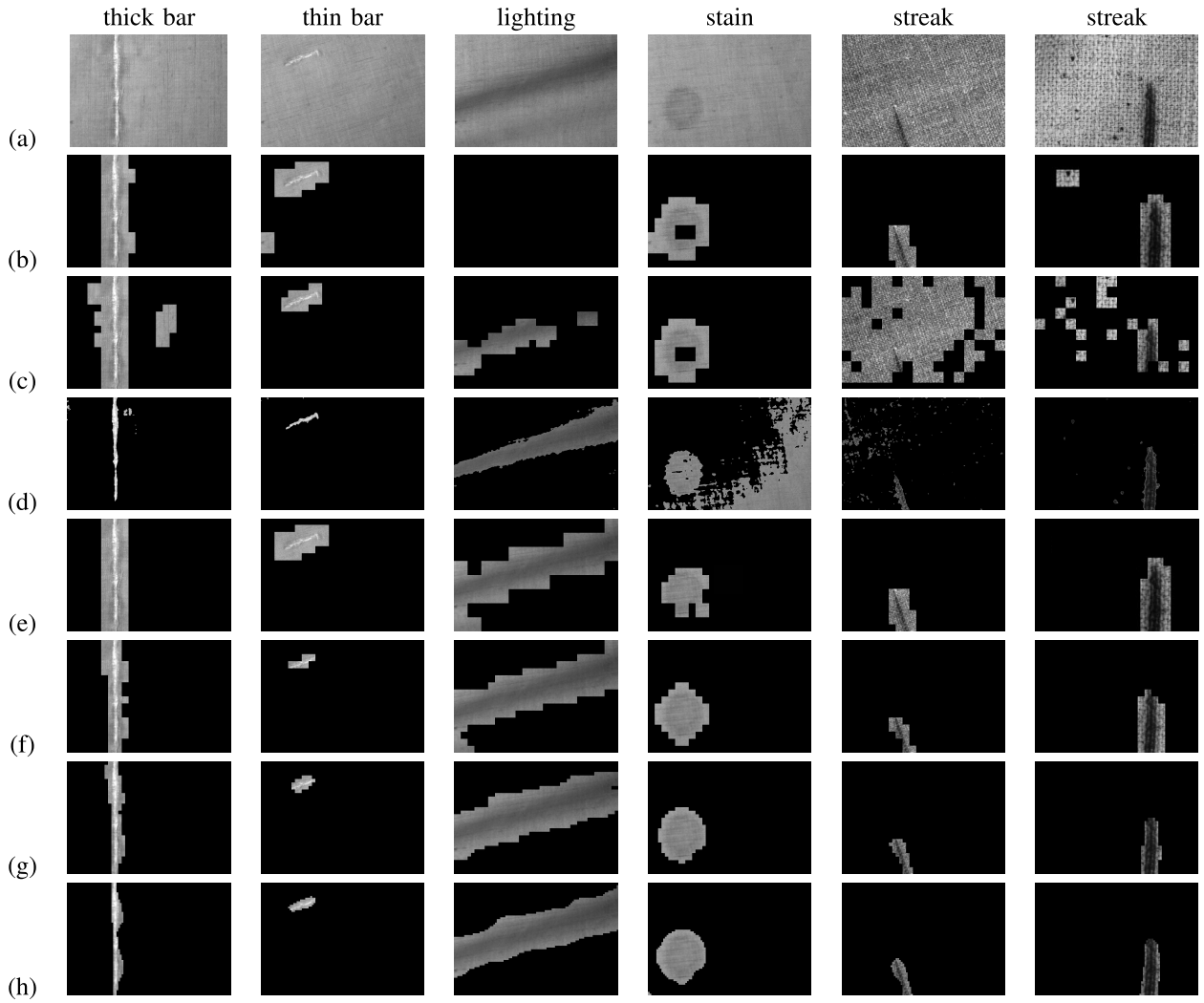

Fig. 8. Comparison of detection results for homogenous fabrics in $p1$ group from classes C1R1 (columns 1–4), C2R2 (column 5), and C2R3 (column 6). (a) Original fabric images. (b)–(e) Results obtained using ICA, LBP, SDD, and RCT-MoGG without overlapping. (f)–(h) Results using RCT-MoGG with $1/2$, $3/4$, and $7/8$ block overlapping, respectively.

pixels (1 for defect and 0 for nondefect). Then, the label having the highest proportion at a given pixel is assigned for its final classification.

In the given example, the original block size is $\mathbf{h} \times \mathbf{w}$ and the desired overlapping is $1/2$ (half) block. This enables having a decision at block size $\mathbf{h}/2 \times \mathbf{w}/2$ for the middle colored block. This is achieved by combining the votes from all the original sized blocks that contain the shaded middle block.

IV. Experimental Results

We have conducted experiments on the popular TILDA database [45]. This database consists of eight types of fabric, which are stored in four class directories {C1, C2, C3, C4}, and each class directory contains two subdirectories. Therefore, each subdirectory contains one fabric type image, each of which are partitioned into 8 subdirectories containing each 50 texture images. The first subdirectory named "E0" contains defect-free images, while the other subdirectories ("E1"–"E7") contain defective images.

TABLE I
Definitions of TP, FP, TN, and FN in Defect Detection

	Actually defective	Actually defect-free
Detected as defective	True positive (TP)	False positive(FP)
Detected as defect-free	False negative (FN)	True negative (TN)

A. Parameter Setting

In the group $p1$ of the data set, most images contain *plain* and *twill* fabrics with texture constituting of very small homogenous patterns. Therefore, we have fixed a block size to 64×64 pixels to allow a reliable estimation of the statistical signatures. In addition, to achieve a good defect localization, the blocks are spatially overlapped as proposed in Section III-D3. For fabrics in the non-$p1$ groups, the block size is automatically calculated by our proposed method in Section III-A. For our study, we have used three homogenous fabric types: C1R1, C2R3, and C2R3 in the $p1$ group and two periodic fabrics: C3R1 and C3R3 in the non-$p1$ groups. Note that C1R1 is a uniform plain fabric, and C2R2 and C2R3

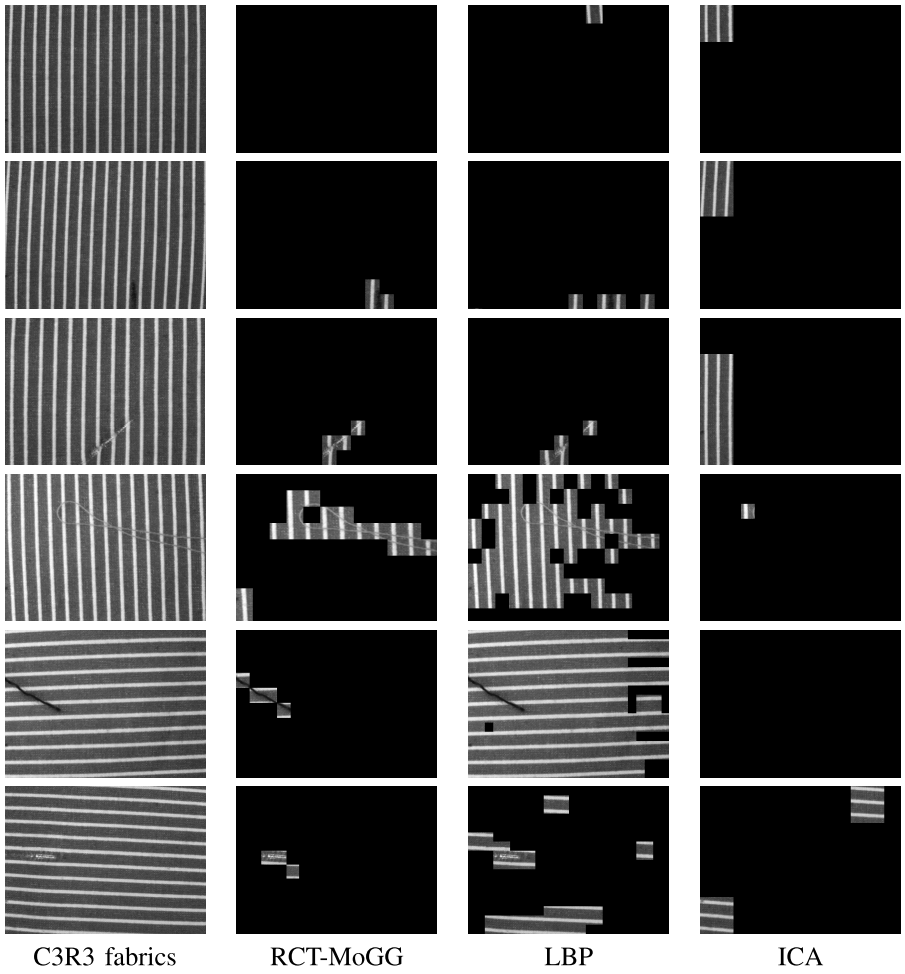

Fig. 9. Comparison of some detection results for striped fabrics.

are *twill* and *plain* weave fabrics, respectively. For the non-$p1$ periodic fabrics, C3R1 and C3R3 are gingham ($p4m$ group) and striped fabrics ($p2$ group), respectively, which have a vertical, horizontal, or oblique orientation.

B. Performance Evaluation Metrics

1) Image-Level Performance Metrics: To be consistent with other methods in the literature, we have first evaluated the performance of our detection algorithm at the image level by calculating detection rates D_R, false alarm rates F_R, and detection success rates (also known as detection accuracy) D_{ACC}. These metrics measure the accuracy of tagging images as containing defects or defect-free. These rates are defined as follows:

$$D_R = \frac{TP}{N_{\text{defect}}} \times 100\% \tag{6}$$

$$F_R = \frac{FP}{N_{\text{defect-free}}} \times 100\% \tag{7}$$

$$D_{\text{ACC}} = \frac{TP + TN}{TP + FN + TN + FP} \times 100\% \tag{8}$$

where $N_{\text{defect-free}}$ and N_{defect} designate the total numbers of defect-free and defective images, respectively. Table I gives the definitions of *true positive* (TP), FP, *true negative* (TN), and *false negative* (FN) in the context of defect detection.

TABLE II

COMPARING THE DETECTION RATE (D_R), FALSE ALARM RATE (F_R), AND THE ACCURACY (D_{ACC}) OF OUR ALGORITHM VERSUS SIMILAR ALGORITHMS BASED ON 50 FABRIC IMAGES IN EACH OF THE FIVE SUBDIRECTORIES (E0–E4)

		C1		C2	
		R1	R3	R2	R3
ICA	D_R (%)	98.5	98	94.5	96
	F_R (%)	**100**	**30**	**52**	**84**
	D_{ACC} (%)	78.8	92.4	85.2	80
LBP	D_R (%)	92.5	94	100	100
	F_R (%)	**36**	**20**	**100**	**100**
	D_{ACC} (%)	87	91	80	80
SSOCBS[58]	D_R (%)	98.5	97.5	97	86
	F_R (%)	-	-	-	-
	D_{ACC} (%)	-	-	-	-
OUR algorithm	D_R (%)	99.5	97.5	96	92
	F_R (%)	**4**	**6**	**10**	**12**
	D_{ACC} (%)	98	96.4	95	91.2

2) Local-Level Performance Metrics: For most of existing methods for defect detection, performance is measured at the image level (i.e., whether an image contains defaults or not). However, such an approach lacks the information about defect localization, which can be important for accessing the accuracy of algorithms. Indeed, even if an image is classified as containing defects by an algorithm, it does not necessarily mean that the right defect is detected. Therefore, we should establish new metrics that can reflect the strength of any method in terms of defect localization.

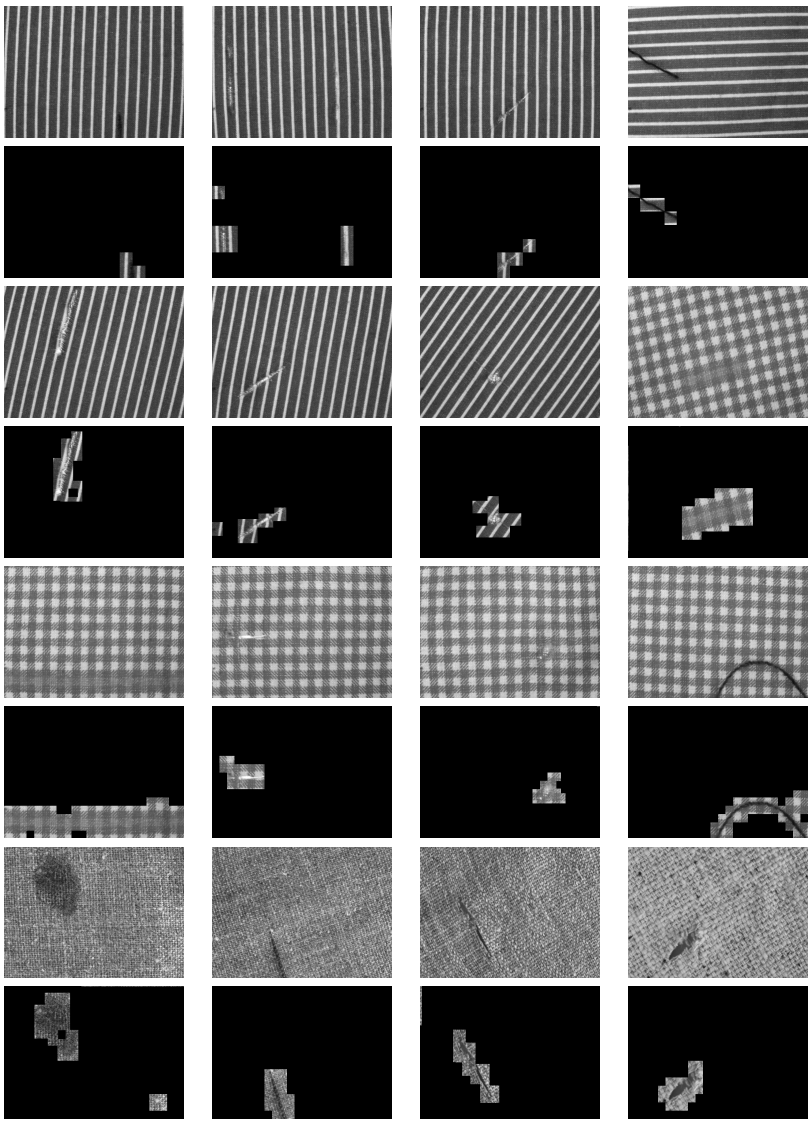

Fig. 10. Examples of defect detection obtained using our approach on fabric images in the TILDA data set. The original images are shown in rows 1, 3, 5, and 7 and are as follows: C3R1 (images –3), C3R3 (images 4–7), C2R2 (images 8–12), and C2R3 (images 13–16). Below each image, we show the detected defects.

In order to evaluate the performance of defect localization, we propose local metrics calculated at the block level of the image, namely, *local precision* (P_L) and *local recall* (R_L), often called *hit rate*. We use also *local accuracy* (ACC_L), which is calculated using local TP (TP_L), TN (TN_L), FP (FP_L), and FN (FN_L) values. TP_L is the number of defective blocks identified as such, TN_L is the number of defect-free blocks identified as such, FP_L is the number of defect-free blocks identified as defective, and FN_L is the number of defective blocks identified as defect free. We define the local *precision*, *recall*, and *accuracy* metrics as

$$P_L = \frac{TP_L}{TP_L + FP_L} \times 100\% \tag{9}$$

$$R_L = \frac{TP_L}{TP_L + FN_L} \times 100\% \tag{10}$$

$$\mathrm{ACC}_L = \frac{2 \times P_L \times R_L}{P_L + R_L} \times 100\% \tag{11}$$

where ACC_L is the harmonic mean of P_L and R_L (balanced mean between precision and recall), which will be used throughout the experiments to assess the merit of the compared methods.

C. Results and Discussion

1) Image-Level Performance Results: We have compared the performance of our method with that of the following defect detection methods: ICA [42], LBP [44], and *slope difference distribution* (SDD) [49]. Note that since SDD is a segmentation method based on histogram thresholding [8], it can be applied only to the $p1$ group. For non-$p1$ groups, this method gives arbitrary results for defect detection.

Fig. 8 shows some results obtained for images in the $p1$ group using ICA, LBP, SDD, and RCT-MoGG with different levels of block overlapping, respectively. We can see that most of methods perform generally well, but the ICA method has failed for the illumination (lighting) defect. Note also that for some images containing small defects (column 5), the LBP method has detected almost the entire image as defective. This is due to the fact that LBP use one experimental threshold that can produce several FPs. In addition, the LBP

TABLE III

COMPARING THE DETECTION RATE (D_R), FALSE ALARM RATE (F_R), AND THE ACCURACY (D_{ACC}) OF OUR ALGORITHM WITH SIMILAR ONES BASED ON FABRIC IMAGES IN EACH OF THE FIVE SUBDIRECTORIES (E0–E4). THE NUMBER OF FABRICS USED FOR DETECTION ARE PUT IN BRACKETS. THE ABSENCE OF BRACKETS MEANS THAT ALL FABRIC IMAGES WITH DEFECTS WERE USED

		C3				
		R1		R3		
		Straight	Oblique	Vertical	Horizontal	Oblique
Our algorithm	$\mathrm{D_R}$ (%)	100 (103)	100 (38)	100 (16)	100 (16)	100 (16)
	$\mathrm{F_R}$ (%)	**9(11)**	**10 (10)**	**0 (8)**	**0 (8)**	**0 (8)**
	$\mathrm{D_{ACC}}$ (%)	99.5 (114)	96 (48)	100 (24)	100 (24)	100 (24)
ICA	$\mathrm{D_R}$ (%)	5 (103)	5 (38)	18 (16)	30 (16)	4 (16)
	$\mathrm{F_R}$ (%)	9 (11)	**20 (10)**	**50 (8)**	**88 (8)**	**87 (8)**
	$\mathrm{D_{ACC}}$ (%)	14 (114)	20 (48)	38 (24)	25 (24)	8 (24)
LBP	$\mathrm{D_R}$ (%)	100 (103)	100 (38)	100 (16)	100 (16)	100 (16)
	$\mathrm{F_R}$ (%)	**55 (11)**	**100 (10)**	**75 (8)**	**40 (8)**	**88 (8)**
	$\mathrm{D_{ACC}}$ (%)	95 (114)	79 (48)	100 (24)	100 (24)	100 (24)

is sensitive to small changes in the structure of the texture patterns. It is worth pointing that the SDD method has proved some accuracy for localizing some defects. However, because the method is based on histogram thresholding [50], it can generate several FPs in the case of nonuniform illumination, for example (see columns 4 and 5). Finally, we can see that our approach has yielded good performance and prevents most of the false alarms. In addition, by applying the block overlapping procedure, our method provides a very good accuracy for localizing the different defects. Fig. 9 shows some examples comparing our algorithm with ICA and LBP on the images of non $p1$ groups (striped fabrics). We can note that our algorithm provides a better accuracy for localizing the defects than the other methods. Finally, some detection results for both $p1$ and non-$p1$ groups are shown in Fig. 10, where we can observe that our algorithm has yielded very accurate localization of defects for all types of fabrics.

For quantitative evaluation, Table II shows the obtained metric values for the homogenous fabrics in the $p1$ group and Table III for fabrics of non-$p1$ groups in the TILDA data set [45]. For this type of fabric, we also included the provided results of the recent method SSOCBS [58]. From Table II, we note that our detection rate, ranging from 90% to 100%, is slightly higher than the three compared methods (ICA, SSOCBS, and LBP). In addition, the detection accuracies of our method on the fabrics C1R1, C1R3, C2R2, and C2R3, which are 98%, 96.4%, 95%, and 91.2%, respectively, are clearly higher than those of the ICA and LBP methods. Note that SSOCBS has not provided figures about the accuracy measure. From Table III, we can observe that the detection rates of our method using fabrics in the non-$p1$ group C3 is 100%. The LBP method exhibits the same result. For these types of fabrics, the ICA almost failed with detection rates ranging from 5% to 30% only. We can also observe for the C3 class in Table III that the accuracy of our method is higher on average, followed by the LBP method, while ICA has the worst performance for this measure.

The most important observation in the above results is the performance of the FRs. Generally, our method generates a lesser number of false alarms than the other methods with both $p1$ and non $p1$ groups (see C1 and C2 in Table II and C3 in Table III). This means that our method has a good capability to accurately recognize an actual defect-free image as defect free. This makes our method more effective since this capability is an attractive property required in the textile industry in order to prevent defect-free rejection. This fact is more emphasized in fabrics of the non-$p1$ group, with 0% to 9% false alarms as shown in Table III. The ICA method is very sensitive in the sense that there are acceptable imperfections (small holes and stains) in texture structure that are not regarded as defects but detected as defective, which causes an increase in FR for some fabrics. This problem is also due to thresholding where small imperfections can disrupt correct detection of defect-free fabrics. Although LBP is more robust than ICA and is a supervised approach, it suffers from the same problem that it is also based on thresholding.

TABLE IV

COMPARING THE LOCAL PRECISION (P_L), RECALL (R_L), AND ACCURACY ACC_L OF OUR ALGORITHM VERSUS SIMILAR ALGORITHMS BASED ON 50 FABRIC IMAGES IN EACH OF THE FIVE SUBDIRECTORIES (E0–E4)

		C1		C2	
		R1	R3	R2	R3
ICA	$\mathrm{P_L}$ (%)	86	85.2	86	78.1
	$\mathrm{R_L}$ (%)	90	88.2	87.1	80
	$\mathrm{ACC_L}$ (%)	**88**	**86.7**	**86.5**	**79**
LBP	$\mathrm{P_L}$ (%)	91.2	93.7	2.1	3.8
	$\mathrm{R_L}$ (%)	80	77	100	100
	$\mathrm{ACC_L}$ (%)	**85.2**	**84.5**	**4.1**	**6.4**
OUR algorithm	$\mathrm{P_L}$ (%)	97.1	95.5	95.8	90
	$\mathrm{R_L}$ (%)	99.5	97.4	95.5	91.2
	$\mathrm{ACC_L}$ (%)	**98.3**	**96.4**	**95.7**	**90.6**

2) Local-Level Performance Results: The performance of the proposed method is evaluated in terms of the metrics: local precision (P_L), local recall (R_L), and local accuracy (ACC_L), respectively. We have also built a ground truth where each block of the tested images is tagged as defective or not defective. Using the same numbers of images as in Tables II and III, respectively, we have compared the performance of our method with that of the other methods (ICA and LBP).

The average values of the local metrics calculated for $p1$ and non-$p1$ groups for each method are shown in Tables IV and V, respectively. Note that small values of R_L indicate that there are many false negatives, whereas small values of P_L indicate the presence of several FPs generated by an algorithm. Compared with the other methods, our algorithm is more effective in defect localization where obtained results with regard to the metric ACC_L values range from (90.6% to 98.3%) for the $p1$ group (see Table IV) and (97.8% to 99.2%) for the non-$p1$ group (see Table V). Compared with our

TABLE V

COMPARING THE LOCAL PRECISION (P_L), RECALL (R_L), AND ACCURACY ACC_L OF METHODS BASED ON FABRIC IMAGES IN EACH OF THE FIVE SUBDIRECTORIES (E0–E4). THE NUMBER OF TEST IMAGES FOR THESE TYPES OF FABRICS IS THE SAME AS THE SPECIFIED IN TABLE III

		C3				
		R1		R3		
		Straight	Oblique	Vertical	Horizontal	Oblique
Our algorithm	P_L (%)	99	98.6	99.2	99	97.5
	R_L (%)	99.4	98.8	99	99	98.2
	ACC_L (%)	**99.2**	**98.7**	**99.1**	**99**	**97.8**
ICA	P_L (%)	4.5	5.6	7.8	9.5	15.2
	R_L (%)	1.1	1.5	1	1	1.1
	ACC_L (%)	**1.8**	**2.4**	**1.7**	**1.8**	**2.1**
LBP	P_L (%)	40.2	25.4	7.1	7.5	5.8
	R_L (%)	85	80.4	77.2	78.6	79.1
	ACC_L (%)	**54.6**	**38.6**	**13**	**13.7**	**10.8**

method, the obtained values of ACC_L by the LBP method, for example, range from 4.1% and 6.4% in fabric C2R2 and C2R3 of the $p1$ group. This clearly indicates that the 100% detection rate (D_R) in Table II does not actually reflect the effectiveness of this method for defect localization in patterned fabrics. Also, the ICA method suffers from missing large parts of the defects in the non-$p1$ group of fabrics (C3R1 and C3R3), where ACC_L has dropped drastically.

V. CONCLUSION

We have proposed a new algorithm that has capability to detect and locate defects in most of the fabric groups. The algorithm uses supervised learning to discriminate between defect-free fabrics from defective ones, based on RCT-MoGG signatures. Experiments on several fabric images have shown that our algorithm yields to good detection rates and very low false alarms. Compared with other methods, the proposed algorithm has shown better performance for *plain*, *plain*, *twill* and *weave* fabrics in the $p1$ group, as well as for the non-$p1$ groups such as *gingham* fabric ($p4m$) and striped fabric ($p2$) with vertical, horizontal, and oblique orientations.

REFERENCES

[1] M. S. Allili, "Wavelet-based texture retrieval using a mixture of generalized Gaussian distributions," in *Proc. IEEE Int. Conf. Pattern Recognit.*, 2010, pp. 3143–3146.

[2] M. S. Allili and N. Baaziz, "Contourlet-based texture retrieval using a mixture of generalized Gaussian distributions," in *Computer Analysis of Images and Patterns* (Lecture Notes in Computer Science), vol. 6855. Springer, 2011, pp. 446–454.

[3] M. S. Allili, "Wavelet modelling using finite mixtures of generalized Gaussian distributions: Application to texture discrimination and retrieval," *IEEE Trans. Image Process.*, vol. 12, no. 4, pp. 1452–1464, Apr. 2012.

[4] M. S. Allili, N. Baaziz, and M. Mejri, "Texture modeling using contourlets and finite mixtures of generalized Gaussian distributions and applications," *IEEE Trans. Multimedia*, vol. 16, no. 3, pp. 772–784, Apr. 2014.

[5] A. L. Amet, A. Ertüzün, and A. Erçil, "An efficient method for texture defect detection: Sub-band domain co-occurrence matrices," *Image Vis. Comput.*, vol. 18, nos. 6–7, pp. 543–553, 2000.

[6] N. Baaziz, "Adaptive watermarking schemes based on a redundant contourlet transform," in *Proc. IEEE Int. Conf. Image Process.*, Sep. 2005, pp. 221–224.

[7] M. Bennamoun and A. Bodnarova, "Automatic visual inspection and flaw detection in textile materials: Past, present and future," in *Proc. IEEE Int. Conf. Syst., Man, Cybern.*, Oct. 1998, pp. 4340–4343.

[8] A. Boulmerka and M. S. Allili, "Thresholding-based segmentation revisited using mixtures of generalized Gaussian distributions," in *Proc. IEEE Int. Conf. Pattern Recongit.*, Apr. 2012, pp. 2894–2897.

[9] C.-H. Chan and G. K. H. Pang, "Fabric defect detection by Fourier analysis," *IEEE Trans. Ind. Appl.*, vol. 36, no. 5, pp. 1267–1276, Sep. 2000.

[10] R. T. Chin and C. A. Harlow, "Automated visual inspection: A survey," *IEEE Trans. Pattern Anal. Mach. Intell.*, vol. 4, no. 6, pp. 557–573, Nov. 1982.

[11] C.-S. Cho, B.-M. Chung, and M.-J. Park, "Development of real-time vision-based fabric inspection system," *IEEE Trans. Ind. Electron.*, vol. 52, no. 4, pp. 1073–1079, Aug. 2005.

[12] F. S. Cohen, Z. Fan, and S. Attali, "Automated inspection of textile fabrics using textural models," *IEEE Trans. Pattern Anal. Mach. Intell.*, vol. 13, no. 8, pp. 803–808, Aug. 1991.

[13] D. E. Joyce. (1994). *Walpaper Groups*. [Online]. Available: http://www2.clarku.edu/ djoyce/wallpaper/seventeen.html

[14] M. N. Do and M. Vetterli, "The contourlet transform: An efficient directional multiresolution image representation," *IEEE Trans. Image Process.*, vol. 14, no. 12, pp. 2091–2106, Dec. 2005.

[15] A. E. Elo, "The rating of chess players," in *Past and Present*. Mountain View, CA, USA: Ishi Press, 2008.

[16] S. Ghorai, A. Mukherjee, M. Gangadaran, and P. K. Dutta, "Automatic defect detection on hot-rolled flat steel products," *IEEE Trans. Instrum. Meas.*, vol. 62, no. 3, pp. 612–621, Mar. 2013.

[17] J.-F. Jing, S. Chen, and P.-F. Li, "Fabric defect detection based on golden image subtraction," *Coloration Technol.*, vol. 132, pp. 1–14, Apr. 2016.

[18] A. Kumar and G. K. H. Pang, "Defect detection in textured materials using Gabor filters," *IEEE Trans. Ind. Appl.*, vol. 38, no. 2, pp. 425–440, Mar. 2002.

[19] A. Kumar and G. K. H. Pang, "Defect detection in textured materials using optimized filters," *IEEE Trans. Syst., Man, Cybern*, vol. 32, no. 5, pp. 553–570, Oct. 2002.

[20] A. Kumar, "Neural network based detection of local textile defects," *Pattern Recognit.*, vol. 36, no. 7, pp. 1645–1659, 2003.

[21] A. Kumar, "Computer-vision-based fabric defect detection: A survey," *IEEE Trans. Ind. Electron.*, vol. 55, no. 1, pp. 348–363, Jan. 2008.

[22] C.-F. J. Kuo and T.-L. Su, "Gray relational analysis for recognizing fabric defects," *Textile Res. J.*, vol. 73, no. 5, pp. 461–465, 2003.

[23] C.-F. J. Kuo, C.-J. Lee, and C.-C. Tsai, "Using a neural network to identify fabric defects in dynamic cloth inspection," *Textile Res. J.*, vol. 73, no. 3, pp. 238–244, 2003.

[24] C.-F. J. Kuo and C. J. Lee, "A back-propagation neural network for recognizing fabric defects," *Textile Res. J.*, vol. 73, no. 2, pp. 147–151, 2003.

[25] R. A. Lizarraga-Morales, R. E. Sanchez-Yanez, and R. Baeza-Serrato, "Defect detection on patterned fabrics using texture periodicity and the coordinated clusters representation," *Textile Res. J.*, pp. 1–14, 2016, doi: 10.1177/0040517516660885.

[26] H. Lee, A. Battle, R. Raina, and A. Y. Ng, "Efficient sparse coding algorithms," in *Proc. Adv. Neural Inf. Process. Syst.*, 2006, pp. 801–808.

[27] M. Li, Z.-M. Deng, and L. Wang, "Defect detection of patterned fabric by spectral estimation technique and rough set classifier," in *Proc. Global Congr. Intell. Syst. (GCIS)*, 2013, pp. 190–194.

[28] A. F. L. Serafim, "Segmentation of natural images based on multiresolution pyramids linking of the parameters of an autoregressive rotation invariant model. Application to leather defects detection," in *Proc. IAPR/IEEE Int. Conf. Pattern Recognit.*, Apr. 1992, pp. 41–44.

[29] G. McLachlan and D. Peel, *Finite Mixture Models*. Hoboken, NJ, USA: Wiley, 2005.

[30] M. Mirmehdi, X. Xie, and J. Suri, *Handbook of Texture Analysis*. Singapore: World Scientific, 2008.

[31] M. K. Ng, H. Y. T. Ngan, X. Yuan, and W. Zhang, "Patterned fabric inspection and visualization by the method of image decomposition," *IEEE Trans. Autom. Sci. Eng.*, vol. 11, no. 3, pp. 943–947, Mar. 2014.

[32] H. Y. T. Ngan, G. K. H. Pang, S. P. Yung, and M. K. Ng, "Wavelet-based methods on patterned fabric defect detection," *Pattern Recognit.*, vol. 38, no. 4, pp. 559–576, 2005.

[33] H. Y. T. Ngan, G. K. H. Pang, and N. H. C. Yung, "Motif-based defect detection for patterned fabric," *Pattern Recognit.*, vol. 41, no. 6, pp. 1878–1894, 2008.

[34] H. Y. T. Ngan and G. K. H. Pang, "Regularity analysis for patterned texture inspection," *IEEE Trans. Autom. Sci. Eng.*, vol. 6, no. 1, pp. 131–144, Jan. 2009.

[35] H. Y. T. Ngan, G. K. H. Pang, and N. H. C. Yung, "Performance evaluation for motif-based patterned texture defect detection," *IEEE Trans. Autom. Sci. Eng.*, vol. 7, no. 1, pp. 58–72, Jan. 2010.

[36] H. Y. T. Ngan, G. K. H. Pang, and N. H. C. Yung, "Automated fabric defect detection: A review," *Image Vis. Comput.*, vol. 29, no. 7, pp. 442–458, 2011.

[37] S. Ozdemir and A. Ercil, "Markov random fields and Karhunen–Loeve transforms for defect inspection of textile products," in *Proc. IEEE Conf. Emerg. Technol. Factory Autom.*, Sep. 1996, pp. 697–703.

[38] G. K. H. Pang, "Novel method for patterned fabric inspection using bollinger bands," *Opt. Eng.*, vol. 45, no. 8, p. 087202, 2005, doi: 10.1117/1.2345189.

[39] S. J. Raudys and A. K. Jain, "Small sample size effects in statistical pattern recognition: Recommendations for practitioners," *IEEE Trans. Pattern Anal. Mach. Intell.*, vol. 13, no. 3, pp. 252–264, Mar. 1991.

[40] C. P. Robert and G. Casella, *Monte Carlo Statistical Methods*. New York, NY, USA: Springer, 2004.

[41] H. Sari-Sarraf and J. S. Goddard, "Vision system for on-loom fabric inspection," *IEEE Trans. Ind. Appl.*, vol. 35, no. 6, pp. 1252–1259, Nov. 1999.

[42] O. G. Sezer, A. Ertuzun, and A. Ercil, "Using perceptual relation of regularity and anisotropy in the texture with independent component model for defect," *Pattern Recognit.*, vol. 40, no. 1, pp. 121–133, 2007.

[43] G. Stübl, J.-L. Bouchot, P. Haslinger, and B. Moser, "Discrepancy norm as fitness function for defect detection on regularly textured surfaces," in *Proc. DAGM/OAGM Symp. Pattern Recognit.*, vol. 7476. 2012, pp. 428–437.

[44] F. Tajeripour, E. Kabir, and A. Sheikhi, "Fabric defect detection using modified local binary patterns," *EURASIP J. Adv. Signal Process.*, vol. 2008, Art. no. 783898, Nov. 2007. [Online]. Available: https://link.springer.com/article/10.1155/2008/783898

[45] *TILDA Database for Textile Defect Detection*, accessed on Feb. 5, 2017. [Online]. Available: http://lmb.informatik.uni-freiburg.de/research/dfg-texture/tilda

[46] I.-S. Tsai, C. H. Lin, and J.-J. Lin, "Applying an artificial neural network to pattern recognition in fabric defects," *Textile Res. J.*, vol. 65, no. 3, pp. 123–130, 1995.

[47] D.-M. Tsai and T.-Y. Huang, "Automated surface inspection for statistical textures," *Image Vis. Comput.*, vol. 21, no. 4, pp. 307–323, 2003.

[48] C. S. C. Tsang, H. Y. T. Ngan, and G. K. H. Pang, "Fabric inspection Based on the Elo rating method," *Pattern Recognit.*, vol. 51, no. 17, pp. 378–394, 2016.

[49] Z. Wang, "A new approach for segmentation and quantification of cells or nanoparticles," *IEEE Trans. Ind. Informat.*, vol. 12, no. 3, pp. 962–971, Mar. 2016.

[50] Z. Wang, "A semi-automatic method for robust and efficient identification of neighboring muscle cells," *Pattern Recognit.*, vol. 53, pp. 300–312, Sep. 2016.

[51] C. S. Wallace, "Statistical and inductive inference by minimum message length," *Information Science and Statistics*. New York, NY, USA: Springer, 2005.

[52] E. J. Wood, "Applying Fourier and associated transforms to pattern characterization in textiles," *Textile Res. J.*, vol. 67, no. 4, pp. 2012–2020, 1990.

[53] X. Yang, K. Pang, and N. Yung, "Discriminative fabric defect detection using adaptive wavelets," *Opt. Eng.*, vol. 41, no. 12, pp. 3116–3126, 2002.

[54] X. Yang, G. Pang, and N. Yung, "Discriminative training approaches to fabric defect classification based on wavelet transform," *Pattern Recognit.*, vol. 37, no. 5, pp. 889–899, 2004.

[55] D. Yapi, M. Mejri, M. S. Allili, and N. Baaziz, "A learning-based approach for automatic defect detection in textile images," in *Proc. IFAC Symp. Inf. Control Manuf.*, 2015, pp. 2423–2428.

[56] J. Zhou, D. Semenovich, A. Sowmya, and J. Wang, "Sparse dictionary reconstruction for textile defect detection," in *Proc. IEEE Int. Conf. Mach. Learn. Appl.*, Sep. 2012, pp. 21–26.

[57] J. Zhou and J. Wang, "Fabric defect detection using adaptive dictionaries," *Textile Res. J.*, vol. 83, no. 17, pp. 1846–1859, 2013.

[58] Q. Zhu, M. Wu, J. Li, and D. Deng, "Fabric defect detection via small scale over-complete basis set," *Textile Res. J.*, vol. 84, no. 15, pp. 1634–1649, Apr. 2014.

Daniel Yapi received the B.Sc. degree in applied mathematics and statistics and applied computer science from the Department of Statistics of Gembloux, Gembloux, Belgium, in 2004, and the M.Sc. degree in statistics from the Institute of Statistics, Université Catholique de Louvain, Louvain-La-Neuve, Belgium, in 2006. He is currently pursuing the Ph.D. degree with the Department of Computer Science and Engineering, University of Quebec in Outaouais, Gatineau, QC, Canada.

He is currently a Lecturer with the University of Quebec in Outaouais. His research interests include machine learning, computer vision, image processing, pattern recognition, and data mining.

Mohand Saïd Allili (M'09) received the M.Sc. and Ph.D. degrees in computer science from the University of Sherbrooke, Sherbrooke, QC, Canada, in 2004 and 2008, respectively.

Since 2008, he has been a Professor of Computer Science with the Department of Computer Science and Engineering, University of Quebec in Outaouais, Gatineau, QC, Canada. His main research interests include computer vision and graphics, image processing, pattern recognition, and machine learning.

Prof. Allili was a recipient of the Best Ph.D. Thesis Award in Engineering and Natural Sciences from the University of Sherbrooke in 2008, the Best Student Paper Award for two of his papers at the conference CRV 2007, and the Best Vision Paper Award at the conference CRV 2010.

Nadia Baaziz (M'05) received the Ph.D. degree in signal processing and telecommunications from IRISA, Rennes I University, Rennes, France, in 1991.

From 1992 to 1995, she was a Post-Doctoral and an Associate Researcher with the INRS-Telecommunications Center, Montreal, QC, Canada. She is currently a Professor at the University of Quebec in Outaouais, Gatineau, QC, Canada. She has served UQO under various administrative capacities, including as Head of the Department of Computer Science and engineering. From 2010 to 2011, she was a Visiting Professor at the Communications Research Center, Ottawa, Canada. Her research interests are mainly in the area of signal, image, and video processing. Research topics include multiresolution analysis, image coding, watermarking and content-based texture retrieval.

Prof. Baaziz is a member of the Quebec Engineer Association Ordre des ingénieurs du Québec, the Canadian Engineering Accreditation Board (2012–2015), and the IEEE Signal Processing Society.